AD-A074 178 MICHIGAN UNIV ANN ARBOR ELECTRON PHYSICS LAB F/G 20/2
ELECTRICAL COMPENSATION IN INP PRODUCED BY BACKGROUND IMPURITIE--ETC(U)
AUG 79 B L MATTES N00019-78-C-0406
UNCLASSIFIED NL

| OF |
ADA
074178

END
DATE FILMED
10-79
DDC

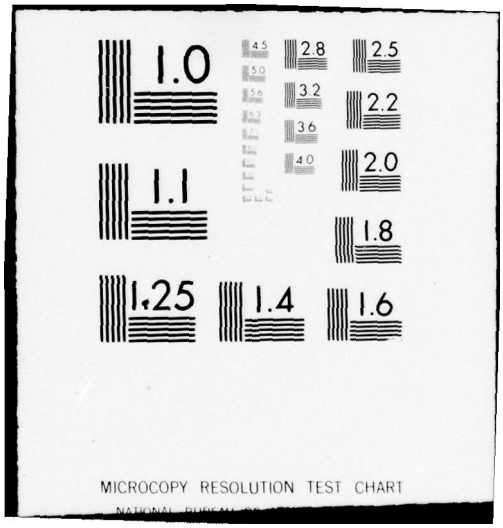
1.0
1.1
1.25
1.4
1.6
1.8
2.0
2.2
2.5
2.8
3.2
3.6
4.0
4.5
5.0
5.6
6.3
MICROCOPY RESOLUTION TEST CHART

(9) Final Report

(6) ELECTRICAL COMPENSATION IN InP PRODUCED BY BACKGROUND IMPURITIES AND STRUCTURAL DEFECTS

Contract No. (13) N00019-78-C-0406

Submitted to

Naval Air Systems Command
Washington, DC 20361

(12) 32 p.

Submitted by (10)

Principal Investigator: B. L. Mattes
Electron Physics Laboratory
Department of Electrical and Computer Engineering
The University of Michigan
Ann Arbor, MI 48109

(11) August, 1979

125 900

ABSTRACT

Liquid phase epitaxial layers of InP have been grown at 475 °C by a steady-state growth technique that maintains the substrate at a constant temperature. The growth system has excellent temperature control, fast thermal response, uniform temperature profiles and up to 50 °C/cm temperature gradients can be induced normal to the substrate. To achieve uniform nucleation on InP substrates at these low temperatures a submersed-displacement cleaning procedure was developed that uses a dilute HCl-methanol etch to remove oxides. The initial layers were discontinuous and had poor electrical properties due to oxide contamination in the In-melt and to substrate oxidation during the heat-up cycle. New In and the covering of the substrate with InP during heat-up appears to have solved this problem. Thermodynamic models of the growth system indicate that the graphite growth cell increases the decomposition of fused quartz and introduces C, O and Si into the In-melt.

TABLE OF CONTENTS

ELECTRICAL COMPENSATION IN InP PRODUCED BY BACKGROUND IMPURITIES AND STRUCTURAL DEFECTS

I. Introduction

Background impurities and structural defects introduced during growth produce compensation, scattering and traps that lower the mobilities in III-V compound semiconductors. The impurities arise from chemical transport reactions between components used in the growth system (fused quartz, graphite and hydrogen).[1] The structural defects arise from substrate surface degradation and lattice mismatch. Therefore, the purpose of this research is to minimize these impurities and defects in the epitaxial growth of InP.

To achieve this goal, a steady-state liquid phase epitaxial (LPE) growth technique, Fig. 1, is being used since growth temperatures below 500 ^{o}C are possible. The advantages of steady-state growth are that the substrate remains at a constant temperature while the rate of growth is controlled by a temperature gradient. The gradient transports the P from a InP source through a P-saturated In-melt. Any desired layer thickness can be grown even though the equilibrium P solute concentration in the In-melt is less than 0.1% at 500 ^{o}C.[2] The lower growth temperatures insure less chemical reactivity, less substrate degradation, and less differential thermal expansion for the growth of heteroepitaxial layers. In addition, the segregation of impurities and dopants can be studied as a function of temperature and growth rate.

The growth system is also being analysed by modelling the chemical transport reactions using quasi-equilibrium thermodynamic calculations to determine the optimum growth conditions to achieve high purity LPE InP.

II. Growth System

The growth system integrated together consists of a semi-transparent furnace with radiant heaters, a heat sink, temperature controls and recorders, a fused quartz reactor tube, a sliding graphite growth cell, and a high purity hydrogen supply. The design and performance of the individual sections will be discussed separately to emphasize the flexibility, control and operation of the system.

A. Furnace

The furnace consists of two independent sources of heat: an external heater which provides an ambient temperature, referenced to a thermocouple immediately below the In-melt for the growth temperature, controlled by a 3-function temperature controller and SCR power supply; an internal heater, arranged above the growth cell to raise the temperature at the top of the In-melt with the InP source, manually powered by an ac variac; and a heat sink, underneath the growth cell that extends the full length of the reactor tube, manually controlled by using a flow of nitrogen gas. The external heater is wrapped longitudinally along the reactor tube and the heat is reflected inwards by a gold-plated pyrex coaxial shield. The radiant heat gives rise to a fast temperature response when temperature changes occur within the reactor tube. The heat sink is used to remove the heat from the internal heater. The internal heater and heat sink induce a temperature gradient across the melt without affecting the growth (substrate) temperature. When the gradient is applied, the temperature perturbation is generally less than a degree for a period of a minute. This design permits growth or substrate temperatures to remain constant while the source (high) and sink (low) temperatures float.

The temperature uniformity over the length of the graphite growth cell (5 cm) varies by several degrees. However, this does

not appreciably affect the growth temperature since the temperature change is quickly corrected as the melt is slid over the substrate. This perturbation has almost been eliminated by using a pyrolytic graphite growth cell.

B. Growth Cell

The graphite growth cell consists of a base to hold the substrate, a slideable boat that contains the InP source and P-saturated In-melt, and a lid to cover the In-melt and InP source. The cell is supported on a quartz cradle attached to the fused quartz reactor cap and when placed at the center of the reactor it rests on the heat sink tubes. Thermocouples are located in fused quartz wells in the lid and base of the cell. The basic design error was that the length of the slideable boat did not cover the substrate during melt saturation. This does not provide a uniform thermal mass to equalize the temperature between the In-melt at one end of the cell and the substrate at the other end. Future modifications will extend the slideable boat over the substrate which will also decrease the growth temperature perturbation when the temperature gradient is applied and prevent substrate degradation.

The well containing the In-melt in the boat was also modified after the first few growths by sloping the vertical walls and increasing the melt contact to overlap the substrate. There is now more In at the top of the melt which forces the melt around the periphery of the boat well base. This correction was also very effective in minimizing melt concection.

During a growth cycle the melt is saturated in a uniform temperature field from the source to the base of the melt. The melt is then slid over the substrate and then the temperature gradient is established to induce P transport from the InP source to the InP substrate, Fig. 2. After a desired thickness has been grown the melt is slid off the substrate and the furnace is cooled down.

C. Reactor Tube

The reactor tube was constructed from GE type-214 fused quartz tubing. The tube is an integral part of the furnace containing internal heater wells, heat sink tubing and thermocouple wells. The thermocouple wells extend into the growth cell and double also as the push-rod to slide the boat. The push-rod and heat sink tubing extend through and are sealed to a fused quartz cap by Cajon Ultra Torr (O-ring seal) fittings. The cap is attached and sealed to the main tube by a 65/40 fused quartz ball and socket joint. The hydrogen is admitted into the reactor tube at the opposite end through stainless steel tubing which is also attached and sealed by an Ultra Torr fitting. All seals are coated with Dow Corning silicone grease. The reactor tube and fittings are, overall, vacuum tight.

The hydrogen is vented between the push-rod and a coaxial tube, which supports the growth cell and is welded to the cap, through a quartz stopcock. The hydrogen enters the annular spacing between the coaxial tubes near the growth cell and flows approximately 30 cm before exitting near the push-rod seal. This purges air that may possible leak through the push-rod seal and backstream into the reactor tube.

The push-rod arrangement works very smoothly. The rod is locked to the sliding boat by a quartz U-shaped bracket. The forked upper and lower thermocouple wells, in turn, lock the lid, boat and base of the growth cell together. The thermocouples in these wells, therefore, travel with the sliding boat to sense the temperature above and below the In-melt.

D. Hydrogen Supply

Commercial standard grade hydrogen is purified in several stages. A 4-tank manifold, with isolation and purge valves for each tank, is connected to a two stage hydrogen pressure regulator. The tanks are replaced when the tank pressure reaches 300 to 400

psi to minimize outgassing products from the tank walls. Following the pressure regulator, operated at 30 to 40 psi, the hydrogen passes through a Deoxo unit to convert any residual oxygen to water and then the hydrogen is filtered and dried to reduce the oil and water vapor content. There are isolation and purge valves before and after each purification stage to leak test, regenerate, and replace every section before reaching a Mathey Bishop hydrogen-purifier. The hydrogen input pressure and temperature of the purifier cell are adjusted to maintain a purified hydrogen flow of approximately 1 l/min to protect the life of the purifier. The pressure in the reactor tube is maintained at 1 psig by throttling the exitting stopcock valve. The hydrogen flow is monitored by measureing the effluent gas with a Matheson #602 flowmeter and a Panametrics hygrometer.

Initially, the reactor tube was vacuum purged by a Vacsorb pump to <10 μm for at least 15 min to prevent air from backstreaming into the hydrogen purifier. Now the hydrogen is allowed to purge the reactor tube continuously when opened and closed to minimize water adsorption from the air.

III. Substrate Preparation

In order to achieve uniform nucleation and growth at low temperatures the InP substrate must be reasonable smooth and flat and, in particular, free of oxides (principally adsorbed oxides like CO, CO_2 and H_2O).

A. Chem-Mechanical Polishing

A Polishing wheel was designed to achieve the three basic motions that create a uniform flat surface. The motions are circular, tangential rotation and translation. These motions are generated by a noncircular block (rounded triangle) which rotates due to friction between the polishing pad and an outer ring on a tilted rotating table. The smoothness of the block

rotation, with circular and radial translation, is adjusted by the tilt angle and the speed of rotation. The polishing surface is a Geoscience pad glued to the rotating table. The block, outer ring and polishing table are high density polyethylene. The polishing solution is 0.5% Br-methanol. The substrates are cemented to the bottom of the block in an "as sawn" condition and then polished. The substrates are polished on both sides to conserve their high cost.

B. Substrate Cleaning

The polished substrates are cleaned by a relatively standard degreasing procedure. First the polished substrate is cleaved to a 1 x 1 cm size and then the surfaces are scrubbed with cotton swabs soaked in detergent. The substrate is then agitated ultrasonically in deionized water. In order to remove the water, the substrate is rinsed thoroughly in acetone three times, and then rinsed in trichloroethylene. The substrate is again thoroughly rinsed in acetone three times and then in methanol. Initially, to remove oxides on the substrate surface, a fresh 1% Br-methanol solution was used. However, a more reliable technique is to use a 1 to 5% HCl-methanol solution to remove the oxides. The solution also imparts a further chemical polish to the substrate. From this stage the substrate is not exposed to the atmoshphere. In order to achieve this, the Br- or HCl-methanol is displaced by successive rinses in methanol followed by isopropyl alcohol, being careful to not expose the substrate to the air. Finally, the substrate is boiled in isopropyl alcohol and withdrawn vertically so that the alcohol wipes, by surface tension, the surface clean and dry. Throughout the cleaning procedure a quartz tweezer is used to hold the substrate until the substrate is placed in the growth cell. The cell with the sustrate is then placed immediately into the reactor tube. Without careful cleaning, in particular the use of a Br- or HCl-methanol solution, uniform wetting by the melt cannot be achieved.

IV. Growths

The steady state liquid phase epitaxial growth system has been used to grow 40 InP layers. Growth temperatures from 400 to 600 ^{o}C have been used, however, most growths were at 475 ^{o}C. The growths, in general, did not have continuous layers due to a variety of problems that ranged from contaminated In to oxidized substrate surfaces. Most of these problems have been minimized and will be discussed in detail.

A. Contaminated Indium

The 6-9's In we recieved from Metals Specialties, which was manufactured by MCP Electronics in England, was contaminated with oxides (In_2O_3 and In_2O). The In contamination was not suspected during the first 30 growths until small black whiskers of In_2O were accidently observed when the In-melt was being replaced. The oxide and other impurities (Si and Al) were identified by an electron microprobe. The concentrations of these impurities must be quite high since the microprobe sensitivity is approximately 10^2 ppm.

Further studies showed that the top of the In ingot (flat surface) was more heavily contaminated than other areas. Direct converstaions with MCP in England revealed that prior to casting the In under vacuum, a "parting" agent is used to release the In from its fused quartz crucible. It is suspected that impurities are introduced during this process and that they concentrate at the top of the ingot because they have lower densities than In. In addition, they pointed out that only "residual resistivity" measurements are used before final casting to monitor the purity of the In.

Based on this information, another source of In was sought which would include a mass spectrographic analysis. Grade A1A In, from Johnson Matthey Chemicals, Ltd. in England through United Mineral and Chemical Corp., was selected. In addition, since the

In wets fused quartz and the latter is a source of Si and O, pyrolytic BN crucibles, purchased from Union Carbide, were shipped to England for casting the In ingot. The same crucibles can be reused for further purchases. The A1A In will be used in new graphite and pyrolytic BN growth cells.

It was found that oxygen contamination of In can readily occur at the melting point of In. Therefore, the melting of In in air is not advisable. A steel chisel is presently being used to size the In for the growth cell. A small furnace will be built in the future to decant the In in a purified H_2 atmosphere. Since In will not wet pyrolytic BN, crucibles and growth cells of this material will be used for handling In.

B. Oxidation of InP

After most growths Newton's rings were observed on the substrate surface where there was poor nucleation. These rings are indicative of a thin oxide. Coupled with the high oxygen contamination in the In and that P has a higher oxidation potential than In, the appearance of 50% P under the In melt will preferentially oxidize the InP substrate. Thus good growths were difficult to achieve. The initial growths were considerably better, however, a bottom section of the In ingot was used.

Note: In general, the quaternaries of In-Ga-As-P are easier to grow on InP than homoepitaxial InP. The reason may be due to the facts that Ga has a higher oxidation potential than P and that As has a reducing potential. Hence the InP will not oxidize as readily by O-contaminated In.

C. InP Substrate Degradation

In addition to the oxidation of the InP substrate, the degradation of its surface prior to growth in the initial graphite growth cell was a problem. Two factors appeared to contribute to the degradation: the substrate was exposed to the reactor environment and to graphite. What probably occurs is the following:

products from the water desorption and the reduction of fused quartz by H_2 (SiO and H_2O) react in the vicinity of the graphite cell to deposit Si and SiO on the substrate. These deposits may act as high energy sites and lead to local decomposition of the InP. This problem has been temporarially overcome by covering the substrate with another InP substrate or a Si substrate prior to growth. Nucleation is now more uniform and there is less degradation. These added substrates must be in close contact and must completely cover the InP substrate. It is anticipated that there will be less degradation when graphite is eliminated by replacing it with pyrolytic BN.

The use of Si in contact with the InP substrate appears to introduce a high concentration of Si into the epitaxial layer, on the order of 10^{19} cm^{-3}, Therefore, InP will be used for high purity growths.

D. Temperature Gradients

The growth of InP by the steady-state LPE process at 500 ^{o}C has revealed several critical factors that influence nucleation and growth. At low temperatures InP is transparent and will not support a temperature gradient, Fig. 2. In order to obtain uniform nucleation extreme temperature uniformity across the growth cell base is required. In addition, the lower the growth temperature, the higher the temperature gradient must be to maintain a high density of nucleation. The temperature uniformity and large thermal gradients up to 50 $^{o}C/cm$ were achieved by using pyrolytic graphite, which has a high transverse thermal conductivity, for the growth cell.

E. Growth Morphologies

The first 10 growths showed regions of continuous growth with fine terraces, Fig. 3. However, there were regions with no nucleation in the form of a cross over the center of the substrate, Fig. 4. It was concluded that some type of solute convection

existed in the melt due to the difference in densities between In and InP, 7.29 and 4.79 g/cm^3, respectively. Attempts were then made to minimize the convection which required the modification of the melt well. The sides were sloped and the base of the melt was widened to extend 1 mm beyond the sides of the substrate. This minimized the apparent convection, however, the melt was also changed which resulted in major nucleation problems-- only hillocks were obtained, Fig. 5. The hillocks were later attributed to the oxidized substrate surface from the oxygen contamination in the In.

Meniscus lines were also observed, Fig. 6. These lines, however, could be eliminated when the melt was "preconditioned" over part of the substrate. The "precondition" procedure consisted of bringing the liquid-solid interface into equilibrium for 5 min or more, with or without a temperature gradient applied, and then sliding the melt over the remainder of the substrate. The remainder of the growth exhibitted no meniscus lines. In addition, no lines were observed when the melt was slid off the substrate. The "preconditionining" may be related to a solute concentration gradient at the interface that must approach pure InP (50% P). Without the "preconditioning" step the melt is in contact with graphite and the P concentration is only about 10^{-3} at 500 ^{o}C. Thus, when the melt is slid onto the substrate the melt is continually trying to establish equilibrium. The InP deposits as lines where the leading edge of the melt at the interface is reaching a 50% composition. This changes the surface tension and depletes the solute in adjacent regions in the melt. The nucleation and growth is thus discontinuous until the solute builds up again.

The uniformity of the layer thickness is very sensitive to transverse temperature gradients. This is due to the rapid change in the P solubility in In at lower temperatures on the order of 10^{-2}, 10^{-3} and 10^{-5} at 600 500 and 400 ^{o}C, respectively. The use of a pyrolytic graphite growth cell, with a high transverse

thermal conductivity, was very effective in minimizing this problem.

V. Layer Evaluation

Van der Pauw measurements are used to determine the carrier density, resistivity and mobility of the epitaxial layer (semi-insulating substrates are used for layer evaluation). An electronic constant current supply (0 to 2 ma) was designed to make four current and voltage measurements between 4 contacts. The contacts are made by pressing 10 mil diameter In spheres at the 4 corners of the epitaxial layer. The layer is mounted in a sample holder with four spring electrodes. For mobility meausrements the layer is inserted into a 2 kG magnetic field. The current and voltages are simultaneously measured.

In addition, Au or Al Schottky barriers can be evaporated on these layers to evaluate their carrier density profiles. Primarily, however, van der Pauw measurements at 77 and 300 ^{o}K are used for evaluation. The 77 ^{o}K mobility measurement will be used to determine the N_A/N_D ratio based on theoretical calculations.

The layer and interface structure will be evaluated by thin film x-ray techniques using a Read camera. In addition, high resolution TEM replication techniques will be used to evaluate the interface between the epitaxial layer and the substrate.

VI. Growth System Reactions

The components of the growth system, principally fused quartz, graphite and hydrogen (denoted as SiO_2:C:H_2), interreact via chemical transport reactions. In addition, fused quartz contains OH radicals and adsorbed H_2O which will desorb when the quartz is heated. The magnitudes of these effects are very critical as they control the background impurity level in the InP epitaxial layers. The water desorption has been monitored and thermodynamic models of the chemical transport reactions have been made.

A. Water Desorption

A Panametrics hygrometer has been attached to the reactor tube output to monitor the H_2O vapor in the effluent H_2. Several observations have been made that indicate H_2O desportion in the vicinity of the growth cell is very critical. Any exposure to air of the internal surfaces of the fused quartz reactor tube significantly increases the H_2O content in the effluent H_2. Therefore, H_2 is allowed to continuously purge the reactor tube when opened. In addition, vacuum purging after closing the reactor tube does not appear to be advisable in that any water vapor present will disperse throughout the reactor. The latter conclusion is based on the result that equal amounts of desorbed H_2O are detected in the effluent H_2 when the reactor tube is locally heated at both ends after vacuum purging. Desorbed H_2O is not observed when the H_2 input end of the reactor tube is heated after the tube has been opened and then closed with continuous purging by only H_2.

An important second observation is that when the reactor tube is locally heated in the vicinity of the graphite growth cell, there is no apparent increase of desorbed H_2O in the effluent gas. This may indicate that the H_2O is reacting with C to form CO. The latter is primarily reponsible for reducing SiO to Si. Thus chemical transport reactions are extremely critical around the growth cell, signifying the need to shield the InP substrate during warm-up preceding the growth.

Water vapor in the effluent H_2 is also observed when the push-rod is slid inwards. However, the increase is slight and backstreaming into the reactor tube is minimized by the exitting H_2 flow.

Water desorption occurs at different rates as the temperature is increased. Heating at a slow rate shows several peaks and inflections, Fig. 7. The rate of desorption is very high up to 80 ^{o}C and then drops off up to 400 ^{o}C and then again increases. These rates of change probably represent different types of

desorption and reactions between the $SiO_2(OH)_x$ with H_2. Controlled bakeouts at these temperatures preceding growth may minimize some of the contamination and substrate degradation.

B. Thermodynamic Models

The composition of the growth system's atmosphere is dependent on the components in the reactor tube and temperature. To determine the composition equilibrium conditions will be assumed and kinetics will be disregarded, except for the case of graphite reacting with H_2 to form methane (CH_4). The latter reaction must be catalyzed to produce an appreciable quantity of CH_4 in a finite period of time. Three models have been analysed to approximate the conditions that exist in the InP growth system. Since H_2O desorbs from the fused quartz the results are presented in terms of fixed initial mole fractions of H_2O to H_2. Other models are still being analysed to determine the effects of P on the stability of fused quartz and the solubility of the reaction products in the In melt.

Case I: Hydrogen and Excess SiO_2

The simplest case to consider is the reduction of fused quartz by H_2 at atmospheric pressure. The treatment is included as a basis to compare other more complex systems that follow. For this case the initial state will consist of H_2 and H_2O with excess SiO_2. The final state will be assumed to consist of only H_2, H_2O, SiO_2 and SiO in equilibrium, given by

$$H_2(g) + SiO_2(a) = H_2O(g) + SiO(g).$$

Note, Case I assumes that elemental Si is not present at equilibrium. The presence of Si will be considered in Case III. The equilibrium constant for this reaction is given by

$$K_{p1} = p_{H_2O} p_{SiO} / p_{H_2}.$$

Under an assumption that $K_{p1} << 1$ and the initial mole fraction of H_2O, $(X_{H_2O})_i$, is << 1, and using a mass balance the partial pressure of SiO is given by

$$p_{SiO} = \tfrac{1}{2}\left\{-(X_{H_2O})_i + \sqrt{(X_{H_2O})_i^2 + 4\,K_{p1}}\right\} .$$

The results are shown in Fig. 8, for the temperature range of interest, where two regions exist:

$$p_{SiO} = \sqrt{K_{p1}} , \qquad (X_{H_2O})_i^2 << 4K_{p1} ;$$

and

$$p_{SiO} = K_{p1}/(X_{H_2O})_i , \qquad (X_{H_2O})_i^2 >> 4K_{p1} .$$

The latter region indicates that only a small fraction of the initial H_2O input is reacted. The $(p_{SiO})_{eq}(I)$ does not decrease with $(X_{H_2O})_i$ until the knee of the curve is reached where

$$(X_{H_2O})_i = \sqrt{K_{p1}} .$$

Case II: Hydrogen, and Excess Fused Quartz and Graphite

The growth system generally includes a graphite growth cell which introduces additional reaction products, C, CO and CO_2, from the following reactions:

$$H_2O(g) + C(\text{graphite}) = CO_2(g) + 2H_2O(g)$$

and

$$2CO(g) = C(\text{graphite}) + CO_2(g) .$$

Again the assumption is made that elemental Si does not form. The respective equilibrium constants for these reactions are

$$K_{p2} = p_{CO}p_{H_2}/p_{H_2O}$$

and

$$K_{p3} = p_{CO_2}/p_{CO}^2 ,$$

respectively.

The application of a mass balance results in the following constraint on the equilibrium partial pressures of the gaseous species

$$p_{H_2O} + p_{CO} + 2p_{CO_2} - p_{SiO} \sim (X_{H_2O})_i .$$

Since the formation of CO_2 is not favored in a strongly reducing atmosphere p_{CO_2} will be neglected. Under such conditions the

equilibrium partial pressure of SiO is given by

$$p_{SiO} = \tfrac{1}{2}\left[-(X_{H_2O})_i + \sqrt{(X_{H_2O})_i^2 + 4K_{p1}(1 + K_{p2})}\right] .$$

The results are shown in Fig. 9, where again two limiting regions exist

$$p_{SiO} = \sqrt{K_{p1}(1 + K_{p2})} , \qquad (X_{H_2O})_i^2 << 4K_{p1}(1 + K_{p2})$$

and

$$p_{SiO} = K_{p1}(1 + K_{p2})/(X_{H_2O})_i , \quad (X_{H_2O})_i^2 >> 4K_{p1}(1 + K_{p2}).$$

Again the equilibrium partial pressure of SiO does not decrease until

$$(X_{H_2O})_i > \sqrt{K_{p1}(1 + K_{p2})}$$

and in addition, only a small fraction of the input H_2O is reacted.

Cases I and II are compared in Fig. 10 as a function of temperature for nearly pure H_2. Note that there is a significant departure for temperatures >600 ^{o}C. The departure arises from the increased reaction between H_2O and graphite to form CO when K_{p2} becomes >>1. The equilibrium partial pressures as a function of temperature for CO, H_2O and SiO are shown in Figs. 11 and 12.

Case III: Hydrogen:Graphite:Fused Quartz System with Silicon

The formation of elemental Si in Cases I and II has been neglected. Important changes in the growth system's atmosphere, however, occur if either Si is formed and/or is in excess. The additional reactions that must be considered are

$$Si(s) + \tfrac{1}{2}O_2(g) = SiO(g)$$

and

$$SiO(g) + \tfrac{1}{2}O_2(g) = SiO_2(s) .$$

If both Si and SiO_2 are present at unity activities, the partial pressures of SiO and O_2 are uniquely determined, i.e., the addition of H_2O will basically have no effect on the equilibrium partial pressure of SiO. The results are shown in Figs. 8 through 12 where the intersections of the Si reaction curve (labled by 2SiO=

Si + SiO_2) with the curves for Cases I and II determine p_{SiO} at different temperatures. When excess Si exists in the reactor tube the p_{SiO} curves are horizontal, independent of $(X_{H_2O})_i$. However, when only Si from the decomposition of the fused quartz is present, the Si will be oxidized for $(X_{H_2O})_i$ greater than at the intersection point and p_{SiO} will decrease as for Cases I and II.

Since the equilibrium p_{SiO} for Case III is below that for Case I up to ~750 °C and over the entire temperature range for Case II, the deposition of Si is thermodynamically favorable. However, this conclusion may not be valid due to uncertainties in the thermodynamic data and kinetic factors may also preclude the actual occurance.

When excess BN is introduced in place of graphite, assuming only the formation of B_2O_3 and N_2, the resulting changes are comparable to Case I.

These results provide some support to the explanations proposed for changes in the electrical properties of epitaxial GaAs.[1] When As-saturated Ga melts were baked out in a graphite boat instead of BN, the transition from n- to p-type conductivity occurred at higher temperatures. This has been ascribed to a high oxygen incorporation from CO into the melt. Case II shows that p_{CO} increases rapidly with temperature becoming important at high temperatures.

Initial treatments of P in the growth system shows that P_4O_6 increases rapidly with H_2O content and it also increases at low temperatures. However, kinetics may play an important role at low temperatures and limit its formation.

VII. Future Plans

The future plans are (1) to proceed with systematic bakeout and growth studies to reach steady state chemical transport reactions in the growth system to achieve epitaxial layers with reproducible electrical properties, and (2) to construct a second growth system for quaternary growths to study the effects of lattice mismatch, thermal expansion differences and interface structure on electrical compensation.

REFERENCES

1. Y. -M. Houng, B. L. Mattes and G. L. Pearson, J. Electrochem. Soc. 125, 2058 (1978).

2. R. N. Hall, J. Electrochem. Soc. 110, 385 (1963).

Thermodynamic Data:

D. R. Gaskell, Introduction to Metallurgical Thermodynamics, McGraw Hill (1973).

G. H. A. M. van der Steen, Philips Res. Repts. 30, 309 (1975).

I. Barin and O. Knacke, Thermochemical Properties of Inorganic Substances, Springer-Verlag (1973).

FIGURE CAPTIONS

Figure 1. Horizontal and vertical temperature profiles for steady-state LPE growth.

Figure 2. Temperature and temperature gradient used for a typical growth at 500 ^{o}C.

Figure 3. Fine growth terraces, #9.

Figure 4. No nucleation due to convection, #11.

Figure 5. Discontinuous hillock growth on an oxidized substrate, #30.

Figure 6. Meniscus lines, #29.

Figure 7. Water desorption from the fused quartz reactor tube heated at 36 ^{o}C/min and then the rate decreased slowly to 23 ^{o}C/min as the 500 ^{o}C growth temperature was approached.

Figure 8. Equilibrium partial pressure of SiO for Case I as a function of the initial mole fraction of H_2O and temperature.

Figure 9. Equilibrium partial pressure of SiO for Case II as a function of the initial mole fraction of H_2O and temperature.

Figure 10. Equilibrium partial pressures of SiO, Cases I-III, for H_2 with very low H_2O content.

Figure 11. Equilibrium partial pressures of CO and SiO for for H_2 with very low H_2O content.

Figure 12. Equilibrium partial pressures of H_2O for H_2 with very low H_2O content.

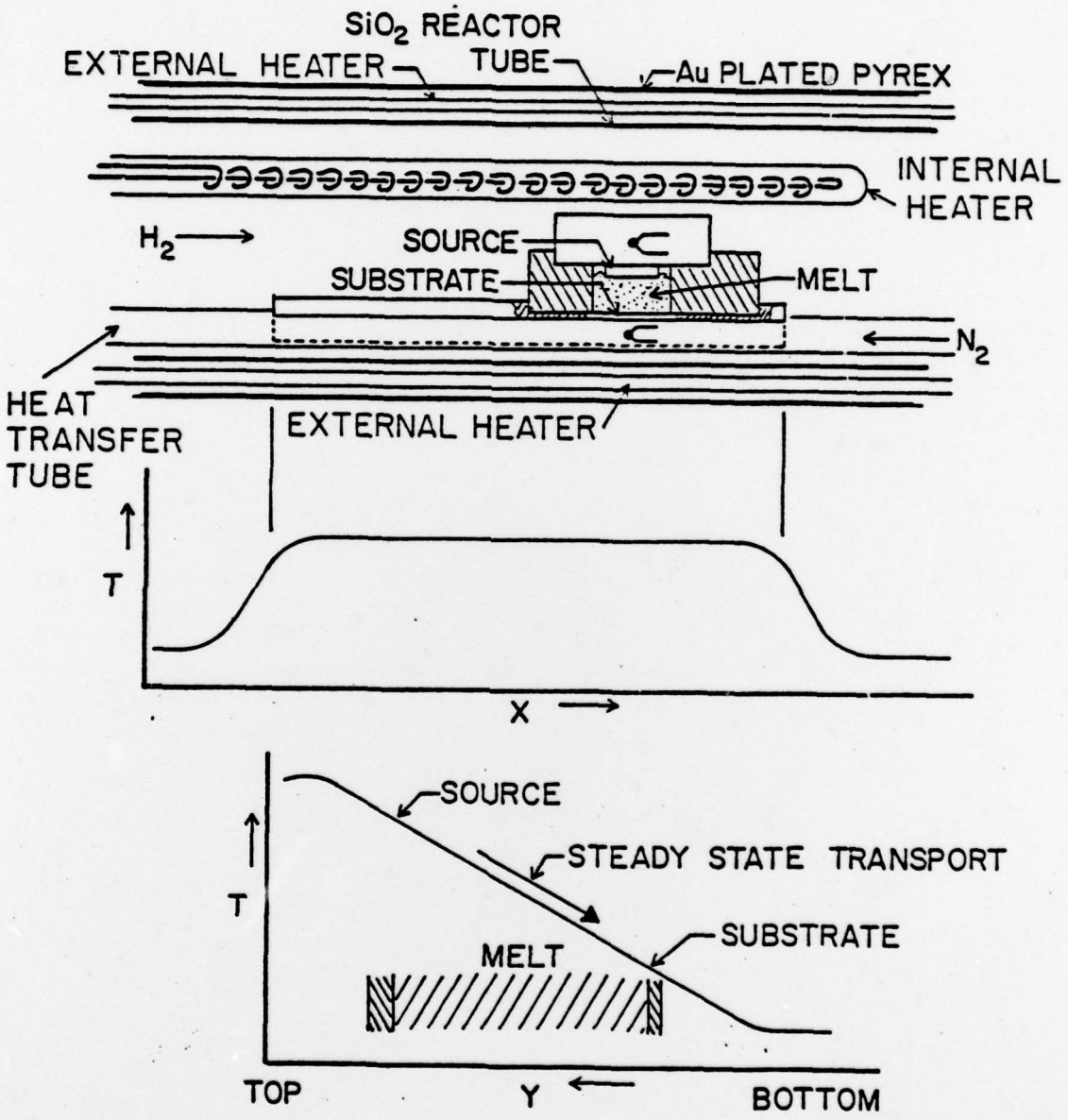

Fig. 1. Horizontal and vertical temperature profiles for steady-state LPE growth.

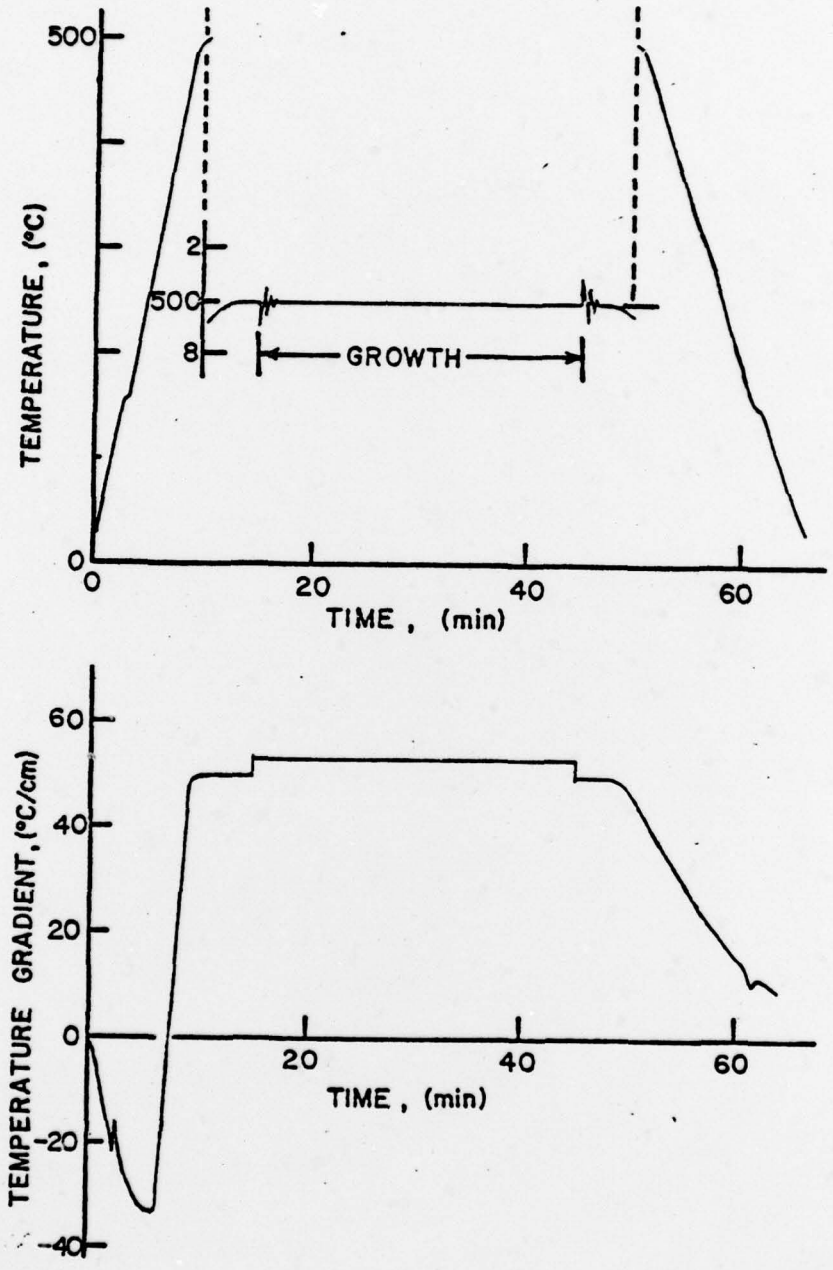

Fig. 2. Temperature and temperature gradient used for a typical growth at 500 ^{o}C.

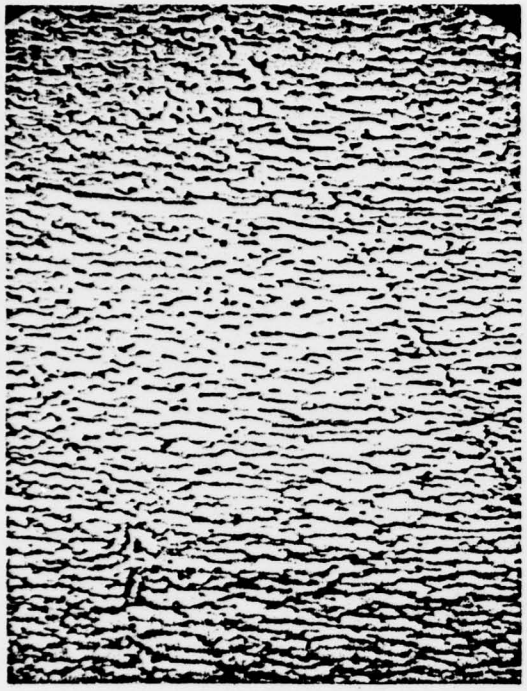

37X

Fig. 3. Fine growth terraces, #9.

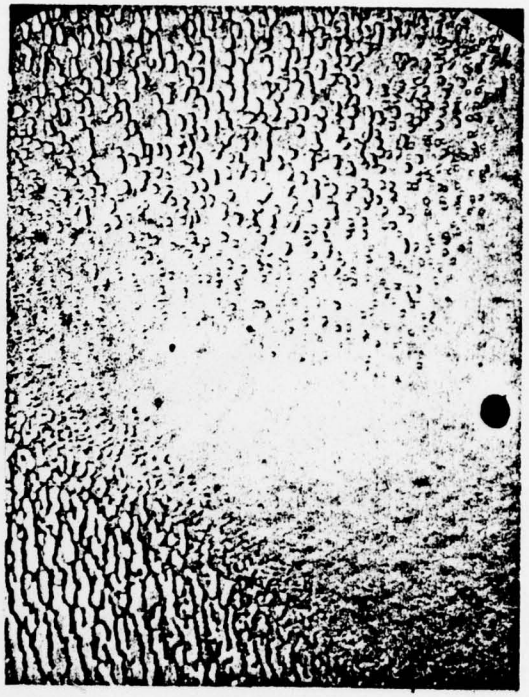

37X

Fig. 4. No nucleation due to convection, #11.

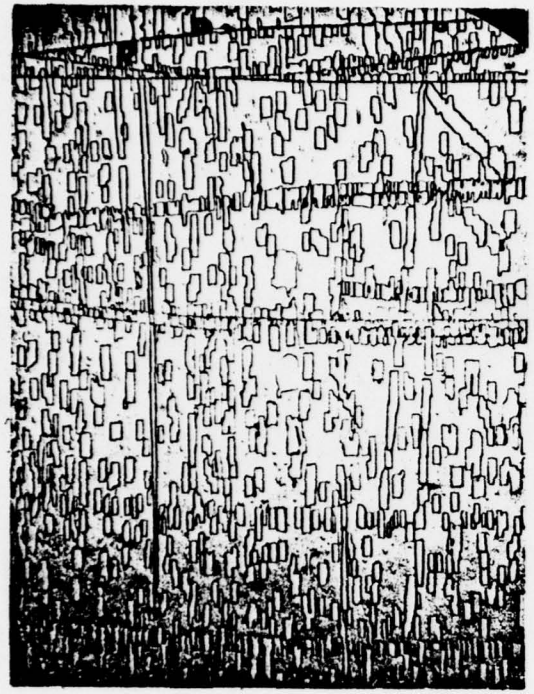

37X

Fig. 5. Discontinuous hillock growth on an oxidized substrate, #30.

37X

Fig. 6. Meniscus lines, #29.

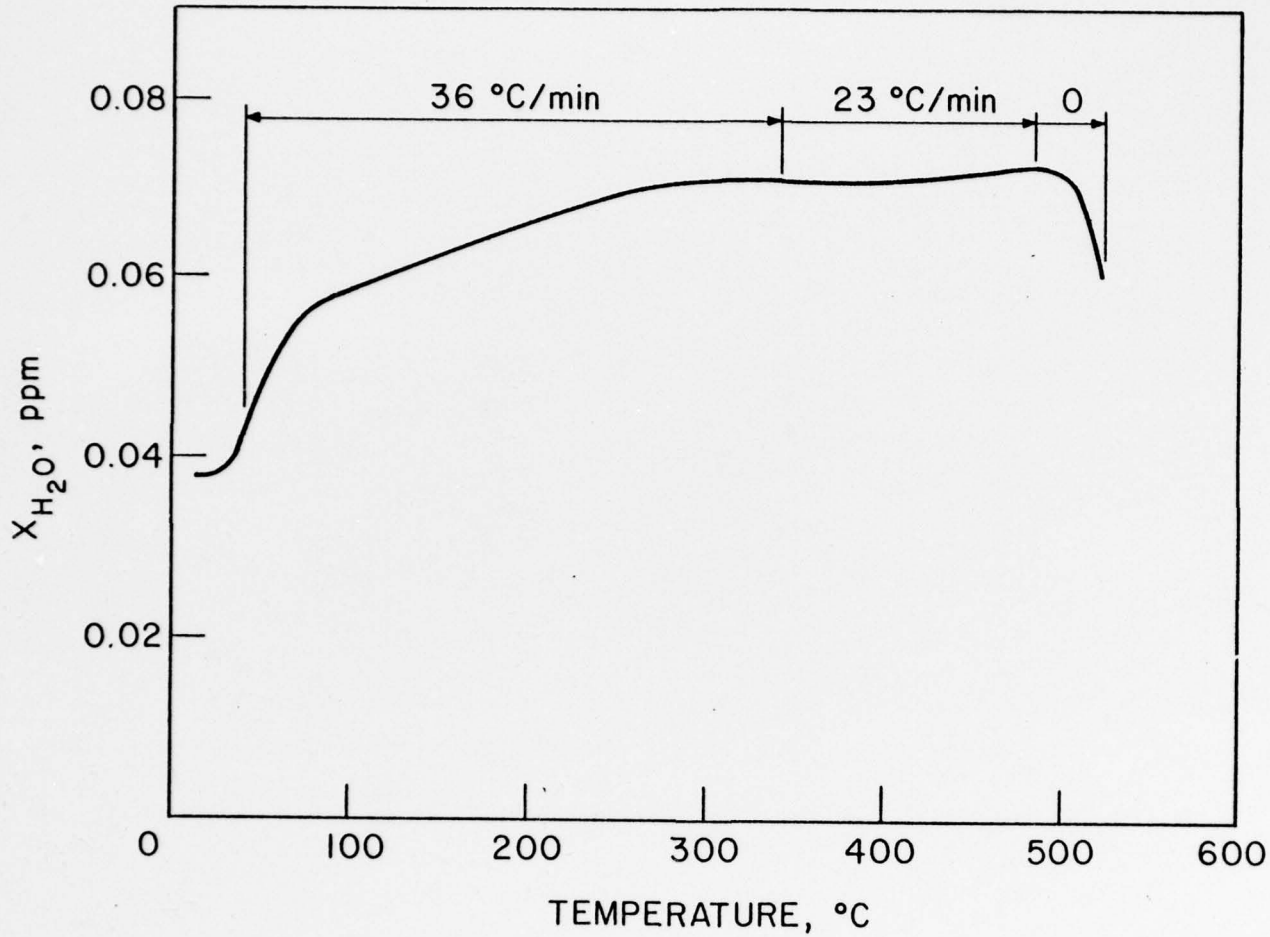

Fig. 7. Water desorption from the fused quartz reactor tube heated at 36 ^{o}C/min and then the rate decreased slowly to 23 ^{o}C/min as the 500 ^{o}C growth temperature was approached.

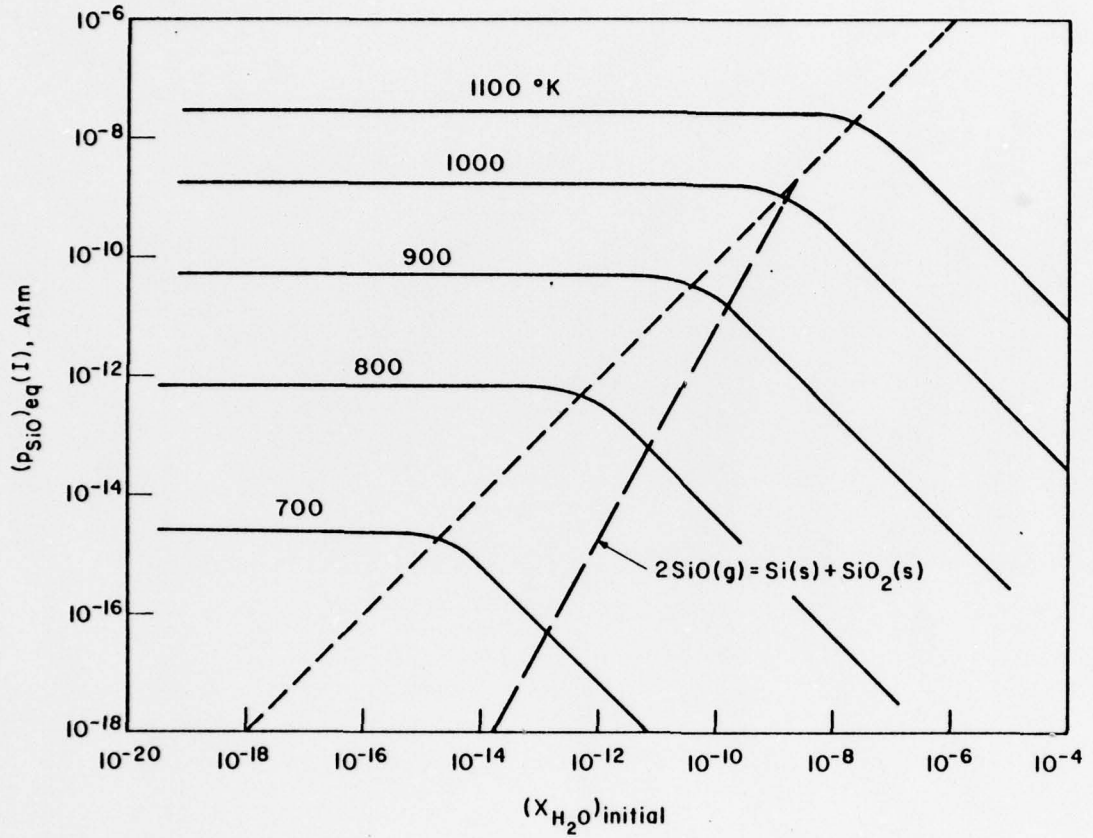

Fig. 8. Equilibrium partial pressure of SiO for Case I as a function of the initial mole fraction of H_2O and temperature.

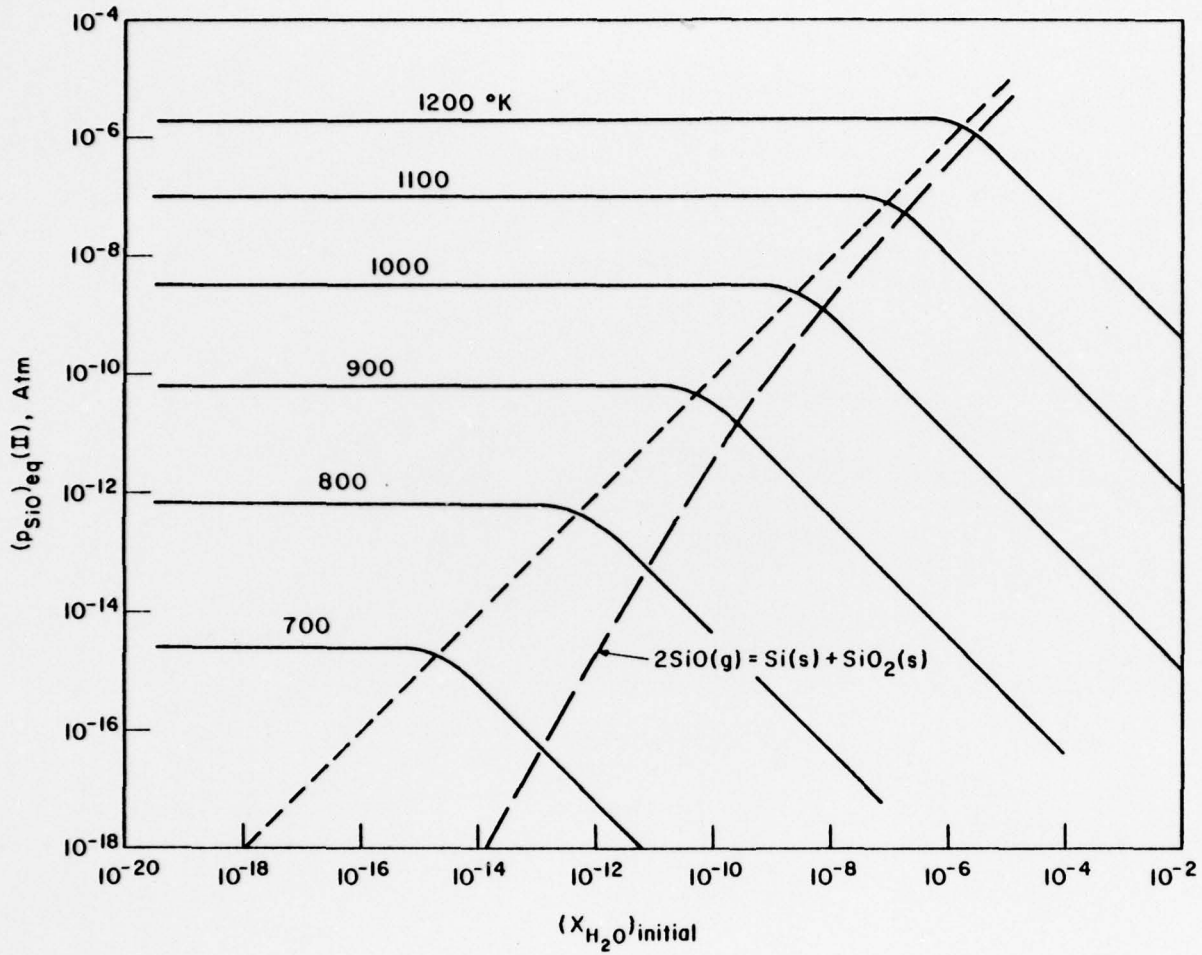

Fig. 9. Equilibrium partial pressure of SiO for Case II as a function of the initial mole fraction of H_2O and temperature.

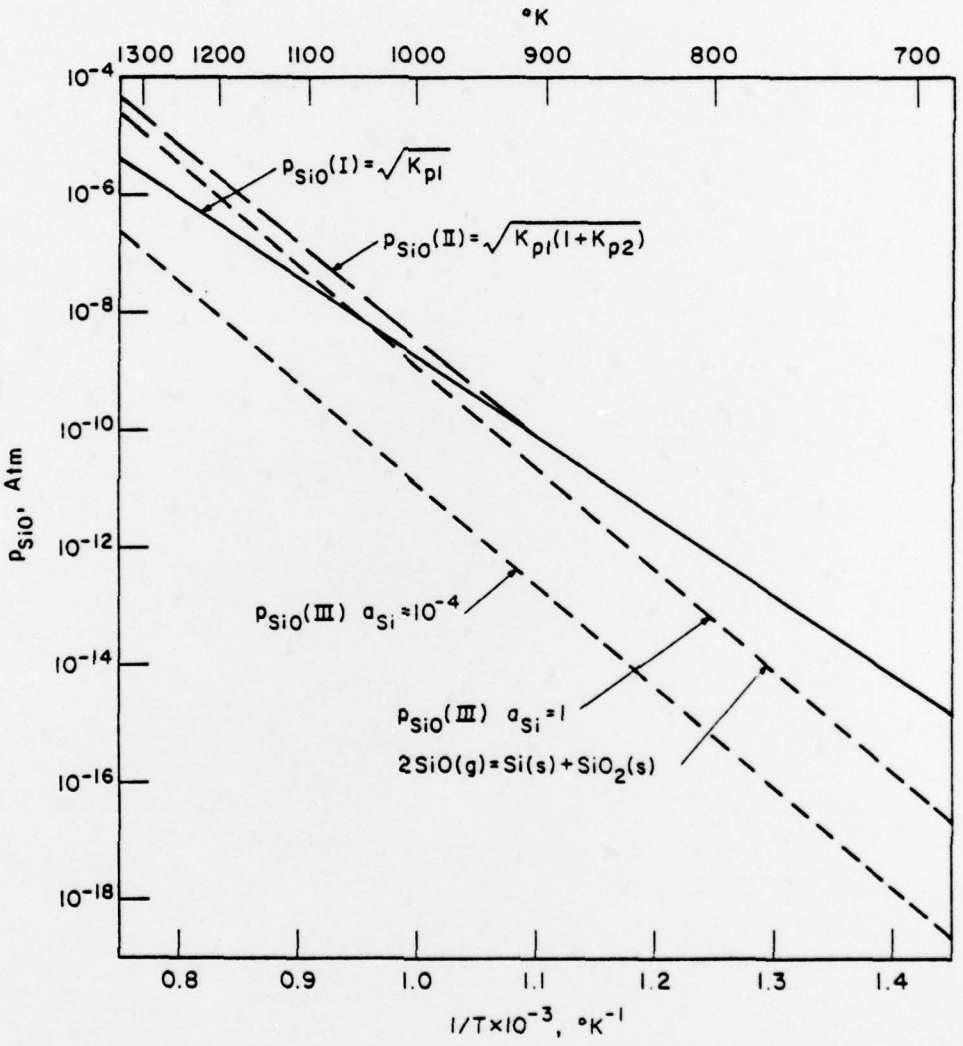

Fig. 10. Equilibrium partial pressures of SiO, Cases I-III, for H_2 with very low H_2O content.

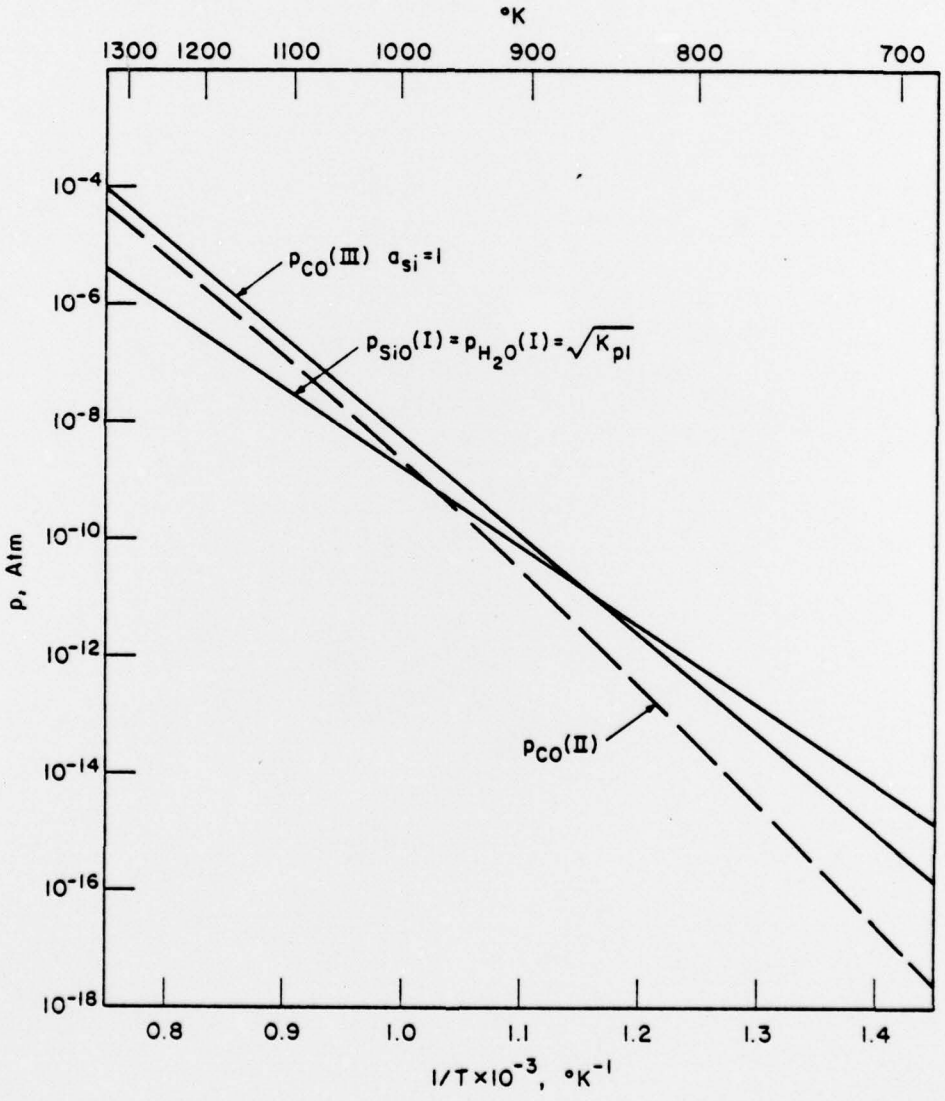

Fig. 11. Equilibrium partial pressures of CO and SiO for H_2 with very low H_2O content.

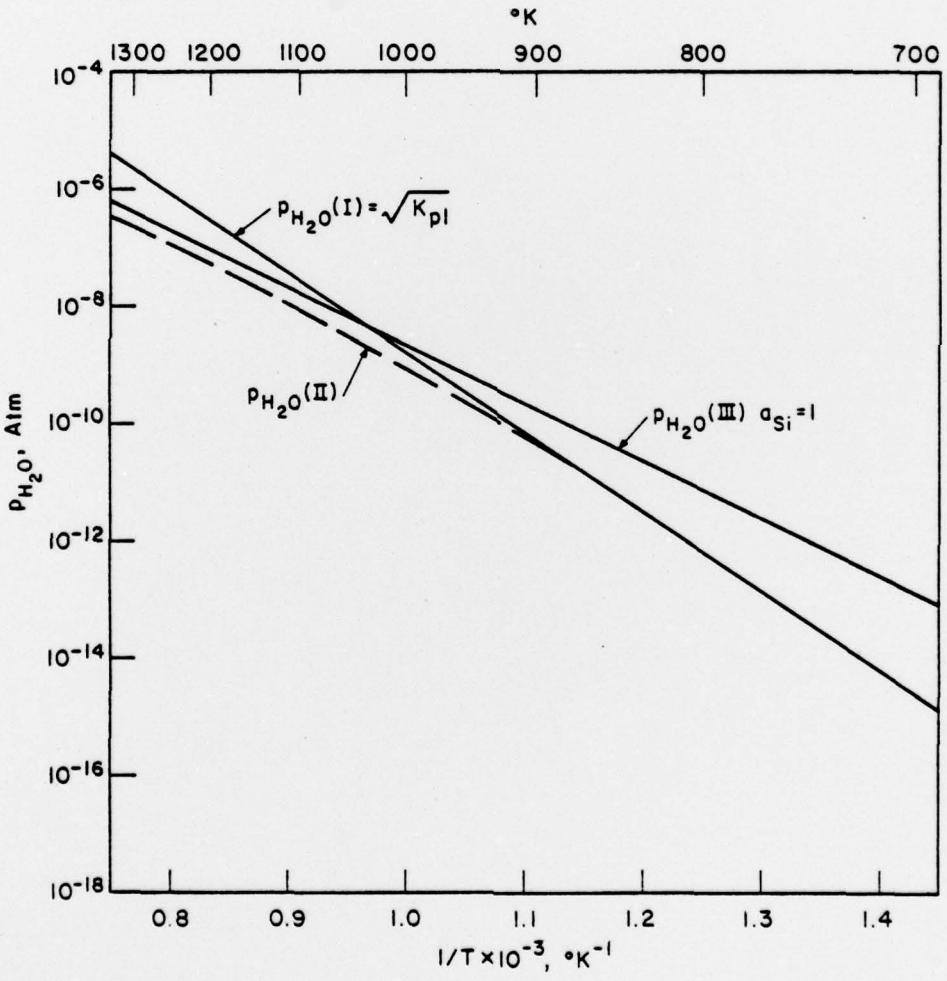

Fig. 12. Equilibrium partial pressures of H_2O for H_2 with very low H_2O content.